ELSEVIER

Contents lists available at ScienceDirect

Journal of Nuclear Materials

journal homepage: www.elsevier.com/locate/jnucmat



The distribution and selective decontamination of carbon-14 from nuclear graphite



Robert N. Worth^{a,*}, Alex Theodosiou^a, William Bodel^a, José David Arregui-Mena^{a,1}, Anthony J. Wickham^b, Abbie N. Jones^a, Paul M. Mummery^a

- ^a Nuclear Graphite Research Group, Department of Mechanical, Aerospace and Civil Engineering, The University of Manchester, Manchester, M13 9PL, United Kingdom
- ^b Honorary Professor, The University of Manchester, Manchester, M13 9PL, United Kingdom

ARTICLE INFO

Article history: Received 29 January 2021 Revised 6 June 2021 Accepted 11 June 2021 Available online 6 July 2021

Keywords:
Nuclear graphite
Nuclear waste
Selective decontamination
Carbon-14
Thermal oxidation

ABSTRACT

This work investigates ¹⁴C release behaviour from UK Magnox reactor sourced irradiated graphite under relatively low temperature oxidation conditions: a 1% oxygen in argon atmosphere at temperatures ranging from 600°C to 700°C, and durations from 4 to 120 hours. A method is used for construction of a detailed ¹⁴C release profile with mass loss. The ¹⁴C release profile is predictable between samples, and an empirical release profile is derived to predict releases to higher mass losses than in this work. An accelerated ¹⁴C release rate at small mass losses is observed, indicative of a ¹⁴C-enriched surface region with a depleting concentration gradient into the material, and the source terms and complexities associated with predicting where the ¹⁴C arose from are discussed. Selective decontamination of a fraction of the ¹⁴C is possible, with the limitation of a reducing efficiency with mass loss and time. This work demonstrates a method for determining the distribution of ¹⁴C between near-surface regions and the bulk material in differing sources of irradiated graphite, and provides data in support of making an informed assessment for the adoption of low temperature thermal treatment and isotopic reduction of irradiated graphite wastes.

© 2021 The Authors. Published by Elsevier B.V.

This is an open access article under the CC BY license (http://creativecommons.org/licenses/by/4.0/)

Introduction

Approximately 97,000 tonnes of the UK radioactive waste inventory, equivalent to 66,000 m³ in volume, consists of irradiated nuclear graphite [1], of which approximately 85% is Intermediate Level Waste (ILW) and the majority of the remainder is Low Level Waste (LLW). The Nuclear Decommissioning Authority (NDA) baseline strategy for irradiated graphite in England and Wales is isolation in a future Geological Disposal Facility (GDF), with Scottish policy endorsing an alternative decision of near surface long-term storage [2]. Strategies for England and Wales include a 'safe storage period' (within the reactor vessel) of the order of 100 years, to allow the activities of shorter-lived radioisotopes to diminish. Irradiated graphite disposal routes in the UK remain under review, however, as there are concerns surrounding whether deep geological disposal is the most appropriate course of action for graphite [2] and timing due to loss of knowledge during any safe storage

period [3]. Alternatives such as thermal treatment of irradiated graphite to achieve selective removal of radioactivity and volume reduction are being explored. This work investigating the selective release of radioactive carbon-14 (14C) under oxidising conditions intends to inform waste management strategies both in the UK and internationally by providing a method for and data pertinent to radioactive release data relevant to thermal treatment of UK Magnox reactor graphites, pre-conditioning of waste assigned to the UK GDF, and potential radioactive release behaviour under accident conditions during graphite reactor dismantling, waste handling and waste storage.

A large proportion of the UK inventory of irradiated graphite waste arises from the now shutdown fleet of Magnox reactors, which utilised Pile Grade A (PGA) graphite as a neutron moderator and structural material in the core. The highest activity radioisotopes produced in neutron-irradiated PGA graphite are ³H, ¹⁴C, ⁶⁰Co and ⁶³Ni [4–6], in reducing order. The activities of both ³H and ⁶⁰Co, with half lives of 12.3 and 5.27 years respectively, will reduce markedly over the safe storage period, and consequently are not of greatest concern for the current strategy of deep geological disposal. The ⁶³Ni inventory, which has a half life of 101 years, will still be present following the safe storage period, though

^{*} Corresponding author.

E-mail address: robert.worth@manchester.ac.uk (R.N. Worth).

¹ Present address: Oak Ridge National Laboratory, One Bethel Valley Road, Oak Ridge, TN, 37830, USA

the radioactive decay is by weak beta emission (maximum energy 66.9 keV) and so does not present the greatest hazard to health. This leaves ¹⁴C, with a half life of 5730 years and maximum beta emission energy of 156 keV, as the dominant persisting radionuclide after this safe storage period, amongst other lower activity long-lived radioisotopes of concern such as 36Cl, which has an associated high energy beta emission of maximum energy 710 keV. Despite the relatively low energy beta emission from ¹⁴C, it is a radioisotope of some concern because of its mobility within the bioand geo-sphere and the consequent risk of wide scale uptake into biological organisms and the food chain [7]. One potential means of reducing this risk of widespread exposure of ¹⁴C is decontamination and separation of the 14C in irradiated graphite prior to final disposal by processes such as thermal treatment, reducing the waste category of the material to LLW and thus achieving a reduction in volume of waste designated for any future GDF. In order for preferential separation to be possible, the ¹⁴C atoms formed must be chemically and/or spatially distinguishable from the remainder of the non-radioactive carbon atoms in the graphite.

This work uses low temperature oxidation of irradiated graphite specimens to demonstrate a method of determining a high resolution ¹⁴C release profile with mass loss, identifies the existence of a ¹⁴C-enriched surface region in UK Magnox reactor specimens, and explores the repeatability and efficiency of removal of that ¹⁴C-enriched surface region.

Background

¹⁴C. Production Pathways and Location

There are two dominant production pathways of ¹⁴C in graphite moderator material, which are from ¹³C and ¹⁴N, which activate to ¹⁴C through neutron absorption interactions. The role of each in contributing to the final ¹⁴C inventory in irradiated graphite is complicated by: varying irradiation histories between reactor designs, individual reactors and locations within a reactor core; large uncertainties associated with the initial impurity content and distribution of the graphite pre-irradiation; the impurity content and influence of the coolant in which it was irradiated; the removal of graphite material through radiolytic oxidation; and the effects of neutron irradiation over sustained periods of time. The neutron absorption cross section of ¹⁴N is approximately three orders of magnitude larger than that of ¹³C, though there is much uncertainty as to the quantity of nitrogen thought to exist in the graphite moderator material. It is known that ¹⁴C production in graphite is highly sensitive to nitrogen impurity levels [8,9], and the level required for production from the ¹⁴N precursor to equal that of ¹³C, which is approximately 1.11% naturally abundant in carbon, is only 7-10 ppm [5,8,10]. There are often differences in the nitrogen levels suggested to be in graphite, ranging from 0.5 to 100 ppm [11,12] and with a recurring assumption of around 10 ppm [5,6], and so it is difficult to predict the contribution of each precursor to the total ¹⁴C inventory [10].

The importance of the contribution from each precursor lies in their initial location within the graphitic structure and the consequent location of the formed ¹⁴C. The ¹³C is homogeneously and randomly distributed throughout the graphite bulk material [13]. The ¹⁴N, abundant in air, could arise from multiple contributions, such as in quinoline insolubles (QIs) from impurities in the source materials during the manufacturing process, it could be trapped within closed porosity, or exist as adsorbed nitrogen at any gas-facing surfaces including throughout the open porosity. This surface-localised adsorbed ¹⁴N component could occur as residual from exposure to air during the graphite manufacture, storage and reactor construction, exposure of the reactor core to air during reactor shutdowns, and as an impurity of the gas phase

reactor coolant [9]. There is also a small contribution to the total ¹⁴C arising in the core from neutron interaction with impurity nitrogen, isotopes of carbon and ¹⁷O in the CO₂ coolant, though this contribution to the ¹⁴C in the moderator material is insignificant [7,9,10,14]. The precursor atom of nitrogen or carbon will likely be displaced from its initial location by the ¹⁴C formation reaction recoil [15], with ion irradiation experiments suggesting an initial maximum displacement of the order of 60 nm for formation from ¹⁴N [16], which has a higher recoil energy than neutron absorption reactions with ¹³C [17]. The effects of any subsequent fast neutron irradiation and collisions with primary and secondary knock-on atoms, which cause damage cascades within the material are unclear [17], though for the purposes of this work any further displacements are likely to be in random directions.

The ¹⁴C atoms that arise from neutron irradiation in graphite could be categorised into one of two populations: bulk ¹⁴C and surface ¹⁴C. For those precursor atoms within the bulk material, the randomly distributed ¹³C and more localised ¹⁴N in QIs, they will be displaced from their original position and then likely be randomly displaced in the structure from further irradiation. Those precursor atoms near the pore surfaces, primarily ¹⁴N and a fraction of the randomly distributed ¹³C, could recoil in any direction upon formation, including both into and out of the graphite, resulting in a concentration gradient of ¹⁴C from the surface inwards, with representative experiments suggesting a typical length scale of tens or hundreds of nanometres into the graphite bulk [14,18]. With progressive irradiation and damage, through natural randomisation, this gradient will likely disperse deeper into the material, though the rate at which it may do so is not clear.

As noted previously, the distribution of ^{14}C at a graphite surface is complicated by contributions from impurities in the coolant. Direct contributions from impurities such as nitrogen and the oxygen and carbon components of the CO_2 coolant gas are difficult to predict [17], though a process of polymerisation of CO in the coolant results in deposition of carbonaceous material onto the surface of graphite [19]. Two separate studies have analysed the deposit on Oldbury Magnox reactor samples using low temperature oxidation and thermogravimetry, 450°C in an oxidising atmosphere, and liquid scintillation counting of the resulting CO_2 to determine the ^{14}C content [20,21]. Each study concluded that the carbonaceous deposit had a substantially elevated concentration of ^{14}C , compared to the underlying material.

Additional complications to estimating the 14C activity and location include the rate and extent of radiolytic oxidation of the graphite, which counters any production of ¹⁴C at surfaces of the open porosity by removal of material, the rate at which any nitrogen at the surface may be consumed, or 'burnt out' (although Metcalfe et al. [10] suggest that this is not significant) and the influence of reactor outages for maintenance whereby the core is temporarily exposed to atmosphere [10] and thus large amounts of nitrogen are introduced. This latter influence may become more prominent with time, as evidence suggests that following neutron irradiation graphite surfaces are capable of adsorbing larger quantities of gas [17], and as such with each successive outage the graphite may be retaining more nitrogen, though some question the likelihood of significant fractions of nitrogen remaining once the CO2 coolant environment has been restored and the reactor resumes operation [17].

Considering the system as a whole, for a ¹⁴C-enriched surface layer to form and persist in the irradiated graphite waste, the rate of deposition of carbonaceous material and production and irradiation-induced dispersion of any nitrogen-derived ¹⁴C at a pore surface must exceed the rate of precursor removal by radiolytic oxidation. A general consensus on this balance for CO₂-cooled reactors has not been reached [22], and is likely to differ between reactor designs, with some authors proposing that ra-

diolytic oxidation dominates and thus the majority of the 14 C is within the bulk material rather than concentrated at open porosity [23].

Thermal Oxidation of Graphite

The thermal oxidation of graphite has been an area of interest for several decades and, as such, has been widely reported in the literature [24–26]. Despite being a complex mechanism, the process may be simplified such that oxygen arrives onto the surface of the graphite where it can either physisorb or chemisorb onto the surface, before reacting with a carbon atom and ejecting as either CO or CO_2 into the gas phase. The temperature, and therefore energy within the system, will play an important role in determining the exact reaction mechanism [27], but several ideas have been put forward leading to either CO production [28] or CO_2 via a multistep process [29–31].

Oxidation of porous carbon materials, including graphite, is known to take place across several regimes of oxidation [24,32,33] with the temperature of the system determining the reaction pathway. Other factors such as graphite density, flow rate of the oxidant, microstructure and impurity content can also be influential [34–36]. There are known to be three regimes, with the transition between each regime being progressive, and the precise temperature range of each regime being dependent upon material properties and experimental configuration. The first regime occurs at relatively low temperatures, and is known as the 'chemical regime'. In this regime, oxidation is dependent on the natural intrinsic reactivity of the graphite, where the transport of oxidant is relatively unimpeded and penetrates through the entire open porosity before reaction occurs at the pore surface. As the temperature increases, oxidation occurs in the second 'in-pore diffusion regime' where a portion of the oxidant is unable to penetrate into the open porosity of the graphite, and the oxidation rate is restricted by the diffusion rate of oxidant and products through the porous network. At higher temperatures, oxidation occurs in the third 'surface boundary layer controlled regime' where elevated temperatures cause exhaustion of the majority of the oxidant at the geometric surface of the graphite, and a boundary layer forms inhibiting oxidant access to the internal porosity and exhaustion of reaction products from the graphite surface [32,37,38]. The consequence of these different regimes, is that the oxidation-induced weight loss at high temperatures occur at the outer geometric surfaces of a sample, whereas, at lower temperatures, carbon is lost predominantly throughout the internal open porosity surfaces, as this is where the largest surface area for reaction is found [38].

Graphite damaged by neutron irradiation exhibits an accelerated rate of thermal oxidation in contrast to unirradiated material [36,39], though this disparity in oxidation rates between irradiated and unirradiated graphite is more pronounced when material is oxidised at lower temperatures such as between 250-400°C.

Since ¹⁴C is chemically identical to ¹²C and ¹³C, this lowest temperature chemical regime of oxidation can be utilised to investigate the existence and nature of a ¹⁴C-enriched surface region at gasfacing surfaces throughout the open porosity in irradiated graphite.

Thermal Treatment of Irradiated Graphite

Many studies considering selective removal of ¹⁴C using thermal techniques have been reported in the open literature, though there are often large differences in the source graphite, irradiation conditions, analytical techniques, applied temperatures and test gases employed. Several of these studies will be summarised here.

Fachinger et al.[40] observed that preferential releases of ¹⁴C could be achieved from treatment of solid and powder irradiated

graphites sourced from the air-exposed thermal column of the FRJ-1 'MERLIN' pool-type research reactor and reflector material from the helium cooled AVR prototype reactor. The experimental arrangement used a tube furnace followed by a bubbler system and liquid scintillation system to determine release fractions, and an inline IR spectrometer to monitor the ratio of CO to CO₂. Treatments were performed at between 870 and 1060°C in flowing argon, although oxygen impurities in the gas phase and some instances of leaks in the system are acknowledged by the authors. Nevertheless, a ¹⁴C to ¹²C release ratio of 14:1 is observed for MER-LIN powder at 1060°C, with higher temperatures proving more effective. One other observation made for this work is that release fractions from samples which had been powdered were lower than those that remained as solid samples, which is thought to be due to the creation of ¹⁴C-depleted surfaces during the milling process.

Data given by Vulpius et al.[41] expand on the results of Fachinger et al.[40] by performing slight adaptations to the experimental arrangement and considering irradiated graphites sourced from the same UK Magnox reactor as this study (Oldbury Reactor 2), the thermal columns of the FRJ-1 research reactor, and the Saint-Laurent UNGG Reactor 2 (SLA2) in France, which is also graphite moderated and CO₂ cooled. High temperature roasting in nitrogen, at 1100°C for Oldbury samples and 1100 and 1300°C for SLA2 samples, released elevated concentrations of ¹⁴C compared to ¹²C removed in the gas phase to a similar degree as observed by Fachinger et al. although with a slightly lower efficiency for SLA2 than Oldbury, and each achieving absolute release fractions of approximately 2.5% of the total ¹⁴C in the sample. This leads the authors to suggest that a large fraction of the 14C in Magnox and UNGG sourced graphites, which have been exposed to the process of radiolytic oxidation over their operating lifetime, is inaccessible to the gas phase. Within the same study, treatment of an Oldbury sample at 900°C in nitrogen with 0.1% oxygen shows considerable releases of ¹⁴C, of nearly 60%, for a corresponding total sample mass loss of 0.7%, suggesting that the addition of oxygen is helpful for selective removal of 14 C. The rate of 14 CO and 14 CO $_2$ production are 'quite linear', and so the authors attribute this ¹⁴C removal to oxidation rather than any diffusion effects. A similar comparison with UNGG graphite is not made, and the authors acknowledge that this high degree of selectivity was not observed in any other experiments. This large release fraction could be the consequence of an undetected carbonaceous deposit, observed on several Magnox samples and thought to be rich in ¹⁴C [20,21]. Despite this anomaly, the experiments by Vuplius et al.[41] indicate the formation of a ¹⁴C-enriched surface region in both Magnox and UNGG sourced graphites.

The mechanism for ¹⁴C production and its subsequent removal have been explored by Dunzik-Gougar et al.[13] who deliberately produced surface ¹⁴C by neutron irradiation of virgin POCO-Foam® graphitic foam samples, and virgin and pre-irradiated NBG-18 grade graphite, all of which had been immersed in liquid nitrogen prior to irradiation. The samples then underwent thermal treatment by oxidation at temperatures of 700, 900 and 1400°C, to explore effects of different regimes of oxidation, using oxygen fractions of 3 and 5% in argon carrier gas. Large relative releases of the deliberately produced ¹⁴C, compared to the ¹²C content, were observed for experiments with oxygen-bearing gases, demonstrating that under these controlled conditions ¹⁴C produced from ¹⁴N could be removed preferentially. Improved release fractions of ¹⁴C relative to the ¹²C content were observed at the lower temperature of 700°C. Thermal treatment in an inert atmosphere of flowing argon was also explored, which also found the relative ratio of ¹⁴C to ¹²C release to be large (195:1 for NGB-18), attributed to oxidation of surface adsorbed oxygen, although absolute release fractions were lower in this case. This work also suggests that using a lower fraction of oxygen in the test gas improves the selectivity of ¹⁴C release, though it is not immediately clear how this correlated with sample mass loss.

Karlina et al.[42] have performed thermal decontamination experiments on Russian RBMK-sourced graphite at 600-650°C in air, and found that selective decontamination of ¹⁴C was effective, with up to 90% of the ¹⁴C released with corresponding sample mass losses of 25-35%. This is likely due to the operating conditions of RBMK reactors whereby the graphite is irradiated in a helium-nitrogen atmosphere, without the corrosive radiolytic oxidation processes of CO₂-cooled reactors, meaning that a large proportion of ¹⁴C could form from the local nitrogen at pore surfaces and remain there.

As previously acknowledged, Metcalfe et al.[20] performed similar air treatment experiments, using a thermogravimetric method and beta liquid scintillation counting, to investigate the activity of ¹⁴C in a reactive carbonaceous deposit layer on the surface of Oldbury Magnox reactor samples, and the activity of ¹⁴C in the underlying bulk material. All samples reported showed a deposit concentration of greater than 10000 µg.g⁻¹, determined by thermogravimetry. A temperature of 450°C is used to slowly oxidise the more reactive carbonaceous deposit, and then a temperature of 650°C is employed to remove the underlying material. The data shows that the average specific activity of ¹⁴C in the gasified material from the initial 450°C oxidation is significantly higher than that from the latter 650°C oxidation step, by a factor of 85. This result is supported by directly comparable results from Payne et al.[21] on similar samples, who observe a large specific activity of ¹⁴C during the 450°C oxidation stage, which is attributed to the deposit, though the authors also acknowledge that surface ¹⁴C formed from ¹⁴N may also contribute. Metcalfe et al.[43] then extend their previous study to include oxidation of Wylfa Magnox reactor samples demonstrating that although the mass fraction of deposit is less prominent in this source of graphite compared to Oldbury samples the associated ¹⁴C content from oxidation at 450°C, attributed to the deposit, is a substantial fraction of the overall ¹⁴C content in a specimen. These works show that selective removal of ¹⁴C from UK irradiated graphite specimens can be achieved using air.

Experiments conducted by Pageot et al.[44] investigated thermal decontamination of UNGG irradiated graphite sourced from Saint-Laurent UNGG Reactor 2 (SLA2) using a CO2 atmosphere to investigate selective decontamination of ¹⁴C. These authors hypothesise that due to radiolytic oxidation removing surface ¹⁴C the majority of the ¹⁴C in this graphite is formed from ¹³C and therefore locked within the graphite structure, and selective removal of ¹⁴C can be achieved by crushing the sample, to expose ¹⁴C rich nano-porosity formed by neutron irradiation damage. This approach is counter to the observations made by Fachinger et al.[40] that solid samples released ¹⁴C more efficiently, though it should be noted that the sample histories are quite different with those of Fachinger et al. irradiated in a pool-type reactor and those from this study[44] irradiated in CO₂ where radiolytic oxidation will have an influence. The authors also use CO₂ as an oxidant in the temperature range 950°C to 1050°C, which is within the first chemical regime of oxidation for the C-CO₂ reaction, and suggest better selectivity of oxidising edge sites, prevalent in higher densities in nano-porosity, can be achieved using CO2 than O2. This work used a thermogravimetric method coupled with beta scintillation counting to establish average ¹⁴C release fractions over discrete time intervals, and found that a 14C to 12C release ratio of approximately 3 can be achieved at 950°C with a corresponding sample mass loss of 2.8%, and this average release ratio can be maintained to a mass loss of 8.2% at 1000°C with corresponding ^{14}C releases of 23.6%. The authors also observe that at 1000°C the selective removal ratio improved from ~2 to ~3 between 3 and 6 hour duration experiments, with the selective removal efficiency reducing again thereafter. This effect has been attributed to evolution of the microstructure from progressive oxidation exposing additional nano-porosity.

For further associated work in this field, additional review material and sources of data can be found in [15, 17, 43] and [45].

Experimental

Sample Provenance

The samples used for this work have been machined from 27 mm thick Pile Grade A (PGA) graphite spacer pieces of an installed 'monitoring' set originally placed inside the core of Oldbury Magnox Reactor 2. This installed set was retrieved in June 2005. An estimated average 40% weight loss has occurred as a consequence of radiolytic oxidation by CO2 in the reactor, accelerated by a titanium tie rod through the centre of the installed set producing a higher local gamma radiation field. Cylindrical cores of approximately 4.5 mm diameter have been machined from the spacer pieces using a bench drill and core drill bit, some of which have been sectioned into two pieces, producing cylinders of between 5 and 12 mm in length. Analysis conducted by the National Nuclear Laboratory (NNL), as per the method described elsewhere [43], found the surface carbonaceous deposit on these samples to be relatively small. The two samples analysed, which were identical in source and form to those used throughout the rest of this study, returned values of approximately 2000 and 2700 μg.g⁻¹ respectively, compared to $10000-25000 \,\mu g.g^{-1}$ in other studies [20].

Thermal Treatment

Apparatus and Method

This work has employed a commercially available Carbolite MTT ³H and ¹⁴C Analyser tube furnace for analysis of radioisotope release during thermal treatment experiments. A schematic of this arrangement can be seen in Figure 1. A pre-mixed bottle of 1 mol.% oxygen in an argon carrier is used as the sample oxidant (BOC, product code 225770), and argon (BOC, 99.998%) is used to provide an inert environment at all times that oxidation is not sought, such as the ramp up to treatment temperature and cool down segment following treatment. A low concentration of oxidant (1 mol.%) has been used to slow the oxidation reaction down compared to using air, and consequently improve the resolution of the ¹⁴C release data. At these temperatures the regime of oxidation is not thought to be affected, though there could be a secondary effect that reduced oxygen concentrations can enhance the selectivity of ¹⁴C removal from irradiated graphite specimens [13], though the extent and mechanism of this is not clear. The flow rate delivered throughout is 100 ± 5 mL.min⁻¹ with ambient conditions of approximately 20-25°C and standard atmospheric pressure. The tube furnace arrangement consists of independently heated sample and copper oxide catalyst zones and four bubblers at the exhaust, arranged in series. The copper oxide catalyst is used to aid oxidation of any 14CO produced into 14CO2 form such that it can be successfully captured in the bubbler train. The first two bubblers (B1 and B2 in Figure 1) each contain 20 mL of 0.1 M nitric acid, for ³H capture in the form of HTO or T₂O, and the latter two bubblers (B3 and B4 in Figure 1) each contain 40 mL of 3-methoxypropylamine, which requires careful handling due to its volatility and flash point temperature of 27°C, for capture of gaseous CO₂ inclusive of ¹⁴CO₂. Aliquots of the radioactive bubbler solution are taken at the end of each experiment for liquid scintillation counting using a Perkin Elmer TriCarb 3100 scintillation counter. Since ³H and ¹⁴C are chemically separated in the bubbler train prior to scintillation counting, and the activity of all other

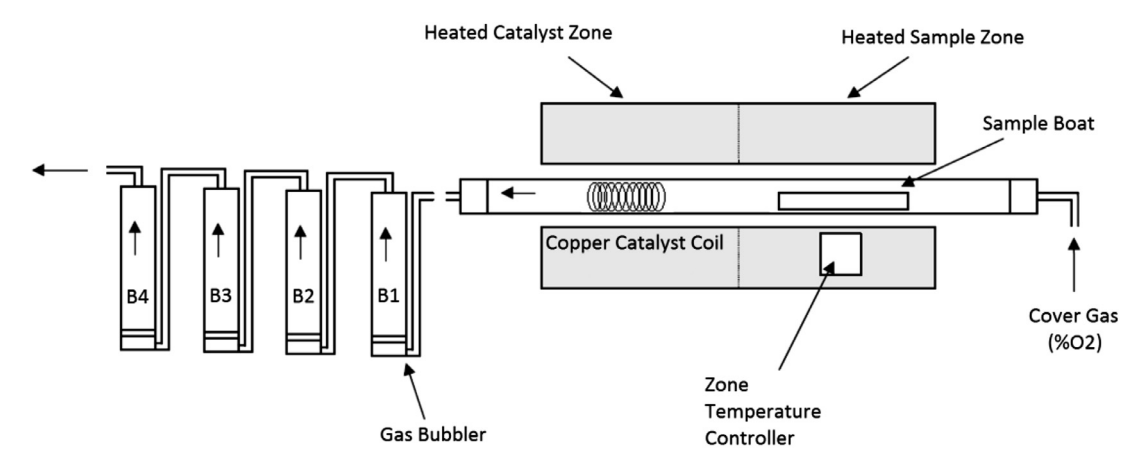


Fig. 1. A schematic of the Carbolite MTT tube furnace and bubbler train arrangement used for this research, adapted from the manual [46].

potentially volatile radioisotopes in irradiated graphite are orders of magnitude lower, interference from other radioisotopes (such as ³⁶Cl) during the counting process is negligible. The experimentally determined radioactive releases are compared to the sample mass loss during the treatment procedure and the total remaining ¹⁴C inventory in the sample, deduced by full oxidation at 1000°C in oxygen at a later juncture, to ascertain the fraction of ¹⁴C released during treatment.

The radioisotope recovery efficiency of this system was checked before and after every four treatment experiments, by replacing graphite samples with known activities of dissolved $^{14}\text{C}\text{-labelled}$ sucrose standards, passed through the furnace and bubbler system to determine the recovery efficiency. The average determined ^{14}C recovery fraction over the course of this work was 95.2 \pm 2.2%. The radioactive releases achieved from irradiated graphite specimens are compensated by this fraction of predictable loss in the system.

Unless otherwise stated, mass losses given in this paper are from the as-received as-irradiated condition, and as such do not incorporate any mass losses incurred during reactor operation.

Experimental Parameters

Phase One of the study employed treatment temperatures of 600, 650 and 700°C for durations between 4 and 8 hours (1 hour increments), in 1% oxygen to assess how the ¹⁴C release efficiency may be affected by varying the temperature and maintaining first regime surface oxidation characteristics. These experiments have been performed on individual samples, and thus each data point produced represents the release characteristics of a different sample, giving an average behaviour between samples. Temperatures between 600 and 700°C were selected because previous experiments show that for these samples first oxidation regime behaviour is induced in this temperature range, which is the regime of interest for selective ¹⁴C removal from near surface regions of the graphite. Samples treated at 800°C oxidised as per the second and third oxidation regimes, exhibiting significant damage to the outer geometric surfaces of the samples.

Phase Two experiments were all conducted at 600°C, also in a 1% oxygen environment, except this time for longer durations extending from 12 to 32 hours of treatment. Combining this approach with Phase One data allows a detailed ¹⁴C release profile with mass loss to be achieved. A practical duration limit of approximately 32 hours has been imposed for these experiments due to natural evaporation in the bubbler train leading to cross-contamination of the ¹⁴C bubblers with ³H-laden nitric acid. This in turn leads to liquid scintillation counting issues, such as chemical incompatibilities and separation of scintillation cocktails with

capture analysis fluids. In a similar manner to the first phase experiments, these experiments are also performed on individual samples, yielding an average behaviour between samples.

Phase Three utilised multiple 600°C treatments of 12 hours each to a single sample on consecutive days, allowing an accumulative 120 hours of treatment to be implemented, which was the maximum duration achieved before the structural integrity was compromised and sample collapse occurred.

Results and Discussion

Phase One and Two Results

The release behaviour of ¹⁴C at different temperatures in a 1% O_2 environment, with increasing mass loss, can be seen in Figure 2. Each data point represents a different sample treated in isolation, up to approximately 9% mass loss. The 14C release profile appears to be broadly independent of temperature, between 600 and 700°C, and approximately linear in nature beyond ~1% mass loss. There is a single potentially anomalous result, at approximately 2% mass loss, included here for completeness, exhibiting a significantly larger ¹⁴C release fraction than similar data points. All of these results exhibit a total ratio of ¹⁴C release to mass loss greater than 1:1. Uncertainties to two standard deviations (2σ) have been determined individually for each data point, by propagation and combination in quadrature of uncertainties from mass measurements, statistical uncertainties in the liquid scintillation counting process, and regular repeatability 'recovery' tests on the furnace. More information on the uncertainty calculations can be found elsewhere [45].

The concentration of ¹⁴C transferred from a sample into the gas phase by thermal oxidation has been established by comparing the total ¹⁴C release for a given sample with the total mass loss induced, giving an average specific activity (Bq.g⁻¹) of that gasified material, which can be seen with respect to sample mass loss in Figure 3. The data show a reducing specific activity of ¹⁴C with increasing mass loss, from approximately 1 MBq.g-1 to 100 kBq.g-1 as treatment progresses. These compare to an average of $56.5 \pm 4.6 \text{ kBq.g}^{-1}$ in these graphite samples, determined by full oxidation and capture of the remaining 14C content for each respective sample. The data appear to be independent of temperature over this 600 to 700°C range, and conform approximately to a reducing power law with an R² coefficient of determination of approximately 0.94, the equation for which is given in Figure 3. The anomalous data point identified in Figure 2 has been excluded for the purpose of curve fitting. As per Figure 2, the uncertainties for Figure 3 have been determined using mass, activity and ¹⁴C re-

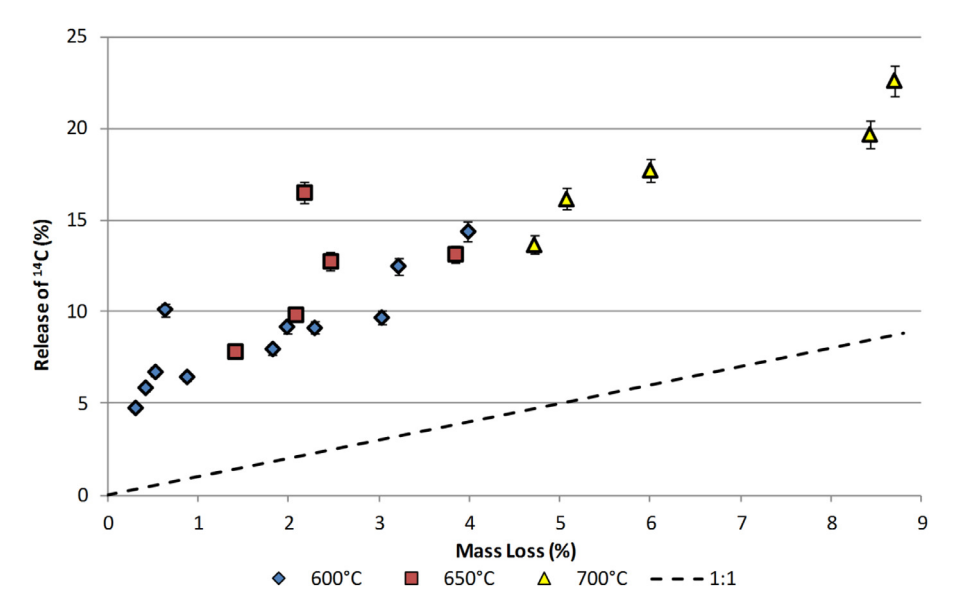


Fig. 2. 14 C releases with mass loss during thermal treatment in a 1% O_2 environment.

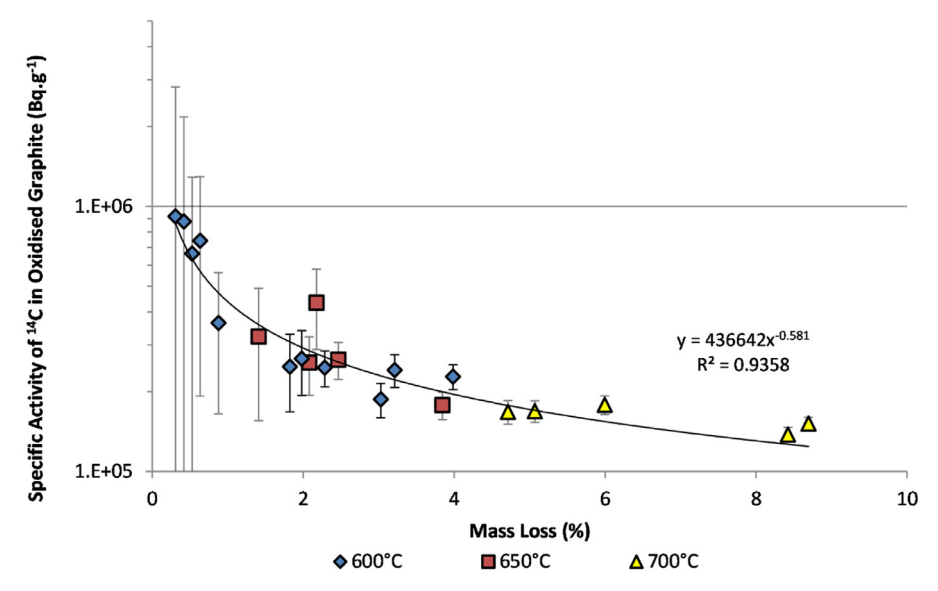


Fig. 3. Specific activity of ¹⁴C in the oxidised fraction of graphite against mass loss, for 21 independently treated samples.

covery data. The error bars associated with small mass losses are large because the mass losses measured fall within the uncertainty of the mass balance and as such cannot be determined with precision. The profile given here is in contrast to data reported for treatment in $\rm CO_2$ by Pageot et al.[44] where improvements in $\rm ^{14}C$ release efficiency are observed during the early stages in the experiment. This could be due to differences in sample provenance, differences between the solid, porous samples used here and the crushed samples used in that study, or between respective treatment atmospheres and temperatures used.

The average rate of mass loss associated with oxidation at 600, 650 and 700°C in this experimental arrangement can be seen in Table 1, where the rate of reaction increases by an order of magnitude, with increasing temperature over this temperature range. The uncertainties given in Table 1 represent two standard deviations of the mass measurements for those datasets. The scatter in the mass loss data associated with 650°C treatments is significantly larger than for 600 and 700°C treatment conditions. The reason for this additional scatter in the 650°C data is not clear, and could be an experimentally-induced artefact due to an insufficient

Table 1 The average rate of mass loss from irradiated graphite specimens during thermal treatment in $1\%~O_2$ at varying temperatures.

Temperature (°C)	Average rate of mass loss $(mg.g^{-1}.h^{-1})$
600	0.90 ± 0.20
650	4.06 ± 1.30
700	10.96 ± 0.93
-	

seal at the ground glass joints resulting in air ingress for those experiments, or natural inhomogeneity in the microstructure and consequent differences in reactive surface area between samples.

Phase Three Results

The results for consecutive treatment of the same sample multiple times at 600°C in 1% oxygen can be seen in Figure 4, allowing collection of thermal treatment data up to mass losses of nearly 25% over 120 hours. The non-linear ¹⁴C release fraction with in-

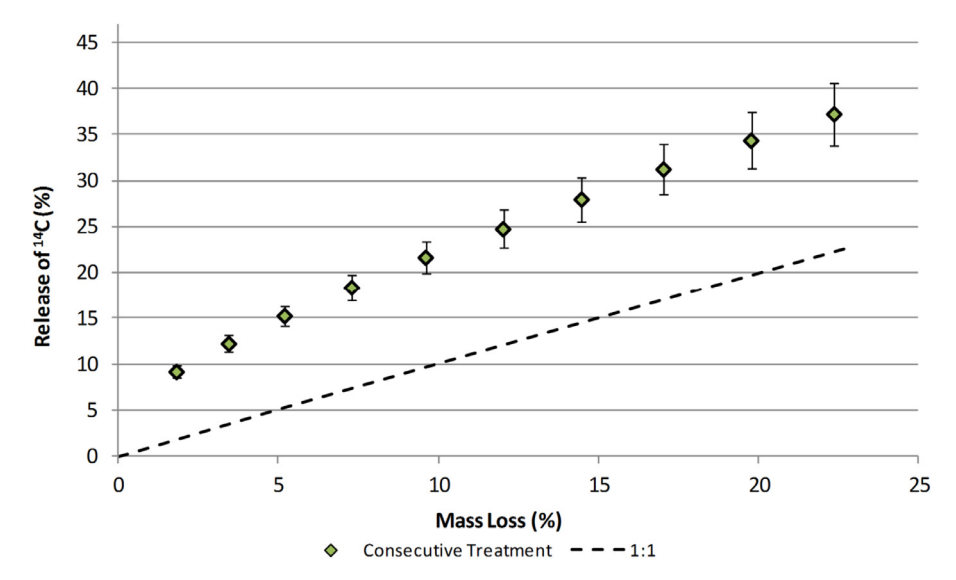


Fig. 4. The release of ¹⁴C against mass loss for a single sample undergoing consecutive treatments at 600°C in 1% O₂.

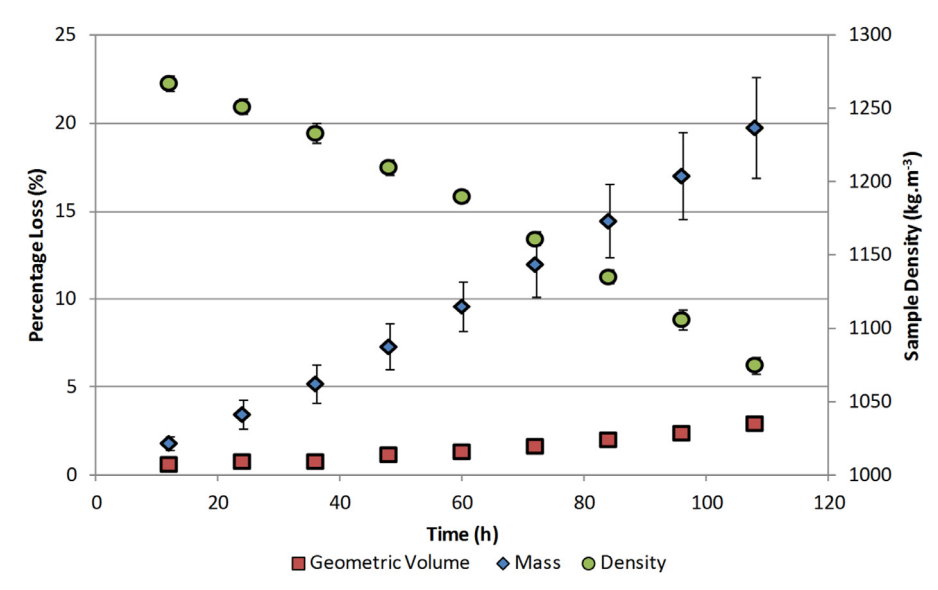


Fig. 5.. Sample geometric volume, mass loss and bulk density with increasing treatment at 600°C.

creasing mass loss agrees with previous data, where the fractional release efficiency remains above 1:1, though that ¹⁴C removal efficiency is decreasing with time and mass loss. Sample integrity was seriously compromised by approximately 24% thermal mass loss (incorporating mass losses during reactor operation this is equivalent to approximately 54% total mass loss from the pre-irradiated condition), resulting in sample collapse during handling. Over 35% of the initial ¹⁴C content had been released into the gas phase before sample collapse occurred. As previously, the uncertainties are calculated by propagation of errors through the measurements taken. In this instance, the error bars are increasing with mass loss because of the accumulation of errors associated with consecutive measurements between treatments.

Sample bulk density information is useful for assessing which oxidation regime has been employed during the thermal treatment experiments. The change in sample mass, geometric volume and bulk density for the sample consecutively treated at 600°C can be seen in Figure 5. With increasing treatment time at this temperature, the sample mass decreases approximately linearly to approximately 20% mass loss, whilst the geometric volume decrease over the same period was approximately 3%, giving a decreasing sample

bulk density with time. The uncertainties have been determined by combination in quadrature of measurement uncertainties as appropriate.

Discussion

Interpretation of the data from Figure 2 to Figure 5 and Table 1 allows information about the ¹⁴C release behaviour from these irradiated graphite specimens to be obtained, including the location of the ¹⁴C in the graphite microstructure, the effects of temperature over this range, the overall ¹⁴C release profile with mass loss for reactor irradiated material, and the repeatability of this ¹⁴C removal process between samples.

The location in the graphite structure from which mass loss is occurring during thermal treatment provides an indicator for the original location of the resultant ¹⁴C release. Relatively low oxidation temperatures have been employed to remain within the first oxidation regime, whereby sample mass loss can be attributed to loss of pore surface material throughout the internal porosity of a sample, although direct observation of this is difficult using these techniques. Various temperature values have been re-

ported for the transition from the first regime towards the second regime in graphite, for several different grades of graphite and experimental conditions, including 550-600°C [47], 600°C [48], 650°C [35,49], 700°C [50,51] and ~825°C (given as 1100K) [52]. Payne et al. [53] have specifically considered the oxidation behaviour of unirradiated specimens of PGA nuclear grade graphite, the same grade as this study, and found first regime oxidation to 600°C. Additionally, the irradiated specimens for this study have a substantially increased porosity fraction compared to virgin material, due to mass losses in-reactor (see Sample Provenance section). A graphite diffusivity study by Hewitt et al. [54] indicates that more porous samples exhibit a much larger gas diffusivity, which in this study on high weight loss specimens is likely to delay the onset of second regime oxidation behaviour, which is limited by in-pore diffusion, compared to the unirradiated study by Payne et al. [53]. To support this assumption, the data in Figure 5 strongly suggests that first regime pore surface oxidation behaviour has been induced at 600°C, by demonstrating that the geometric volume of the sample reduced by approximately 3% as the sample mass reduced by nearly 20%, meaning that the majority of the mass loss is occurring within the sample and not from external geometric surfaces as per the third oxidation regime. These comparisons with literature and supporting data suggest that first regime oxidation has been achieved in this work. The 600°C treatment data in Figure 3 show that the specific activity of ¹⁴C released into the gas phase by oxidation is initially large, approximately a factor of 20 larger than the average specific activity in the whole sample. There are three potential contributors to this effect: thermal diffusion of mobile ¹⁴C to the gas-facing surface; preferential oxidation of a $^{14}\mathrm{C}$ rich carbonaceous deposit; and progressive removal of a ¹⁴C concentration gradient formed from ¹⁴N at pore surfaces. Considering these in turn, it is possible that during prolonged periods at elevated temperatures ¹⁴C atoms that reside in 'displaced' locations within a damaged lattice may be more mobile and able to diffuse through the material. Experiments by Kanter [55] and Sach and Williams [56] demonstrated that diffusion of ¹⁴C in graphite is slow even at temperatures of 2200°C, albeit in graphite which has not experienced bulk scale neutron irradiation damage. For this work, inert atmosphere tests with Oldbury Magnox reactor samples at 700 and 800°C (not shown here, given in[45]) indicate a very slow release of ¹⁴C into the gas phase which is attributed to inevitable oxygen impurities in the test gas flow. Similar observations have been made by Pageot et al.[44] considering releases of ¹⁴C in He at 1000°C, where they state that the activity remains unchanged within a 3% uncertainty threshold. Thermal diffusion of ¹⁴C to gasfacing surfaces is therefore not thought to be a significant contributor in this instance. Previous studies considering the activity of ¹⁴C in carbonaceous deposits on graphite [20,21] have found that these layers are enriched with ¹⁴C, with specific activities of the order of 10⁷ Bq.g⁻¹ observed [20]. It is difficult to completely decouple the ¹⁴C in the deposit from any contributions of the underlying graphite material using thermogravimetric techniques due to oxidation of both components, although Metcalfe et al.[20] indicate a strong correlation between samples with large deposits and ¹⁴C released through thermal treatment. This suggests that the deposit content on the samples tested in this study, though smaller than seen elsewhere, may have influenced the results. The mass fraction attributable to the deposit in these samples, based on measurements at NNL, is around 0.2-0.3%. If the trend in Figure 3 is extrapolated backwards, the specific activity at these low mass losses is likely to be large, greater than 10⁶ Bq.g⁻¹, though elevated fractional releases of ¹⁴C to ¹²C continue to much higher mass losses than can be attributed solely to the deposit. Therefore, assuming that graphite removal is uniform across all gas-exposed surfaces at 600°C, and the 13C-derived 14C component is randomly distributed, it is likely that the remainder of the ¹⁴C release profile is attributable to a decreasing concentration of ¹⁴C with increasing depth into the bulk material and a 1:1 release of ¹³C-derived ¹⁴C with mass loss. This provides evidence for a ¹⁴N-derived ¹⁴C-enriched surface region which depletes with additional oxidation, though similarly to the development of a ¹⁴C concentration gradient from nitrogen, it is also plausible that some of the ¹⁴C in a surface deposit could be forced deeper into the structure by neutron irradiation. It should be reiterated that this trend is observable from a study including samples which have been exposed to an accelerated rate of radiolytic oxidation (see Sample Provenance section), and thus the surface ¹⁴C concentration effect and concentration gradient will likely be more pronounced in trepanned samples from a similar region in the core.

It can be seen from continuity in the trends in Figure 2 and Figure 3 that increasing the temperature to 650 and 700°C does not significantly influence the ¹⁴C release characteristics in these samples, except for increasing the rate of removal as per the oxidation rate data in Table 1, suggesting that an increase in temperature can induce a similarly efficient ¹⁴C removal process in less time. It is plausible that the transition from the first oxidation regime towards the second in pore diffusion dependent regime (and consequent reduction in ¹⁴C removal efficiency) is occurring at higher temperatures than might be expected from experiments with unirradiated material, as discussed above, or alternatively the true influence of temperature is masked here by inhomogeneity between samples and small sample sizes.

Application of a demonstrative linear trend line to Figure 2 and extrapolation of this trend to the extremes of 0% mass loss and 100% mass loss show that a fast release of ¹⁴C must have occurred earlier in the experiments. The data presented in Figure 3 support this assessment that faster ¹⁴C release rates are observed earlier in the experiments as there is a sharply declining specific activity in the gas phase with sample mass loss, conforming approximately to a reducing power law. Despite limitations with equipment resulting in large uncertainties for small mass losses, it can be confidently asserted that the mass losses are small and the associated specific activities in the early stages of the treatment process are large compared to the remaining material.

Returning to the concept outlined in the introduction of two populations of ¹⁴C (one randomly distributed through the bulk material and the other as a ¹⁴C-enriched surface layer), as the transition from oxidation of surface region ¹⁴C to oxidation of evenly distributed ¹⁴C occurs with increasing mass loss the ¹⁴C release profile will transform from the reducing power law, as per the trend line fitted to the data of Figure 3, to a more linear response representing oxidation of the randomly distributed ¹³C-derived ¹⁴C found in the bulk material. Using the power law shape function fitted in Figure 3, based on the release behaviour of 21 samples offering confidence and resolution, an empirically estimated release profile incorporating both power law and linear trend components into higher mass losses can be derived by solution of simultaneous equations. The equation solved is of the form seen as Equation (1), where *A* and *B* are coefficients to be determined.

$$y = Ax^{0.581} + Bx ag{1}$$

A suitable second coordinate for the simultaneous equations is selected from the data points close to the imposed trend line in Figure 3, corresponding to 24 hours treatment at 600°C and approximately 3% mass loss. The solved empirically derived equation can be seen as Equation (2).

$$y = 4.588x^{0.581} + 0.334x \tag{2}$$

The resultant predicted ¹⁴C release profile during first regime thermal oxidation to complete sample destruction is plotted in Figure 6, alongside a demonstrative 1:1 ¹⁴C release to mass loss line which reflects the expected ¹⁴C release profile if a ¹⁴C-

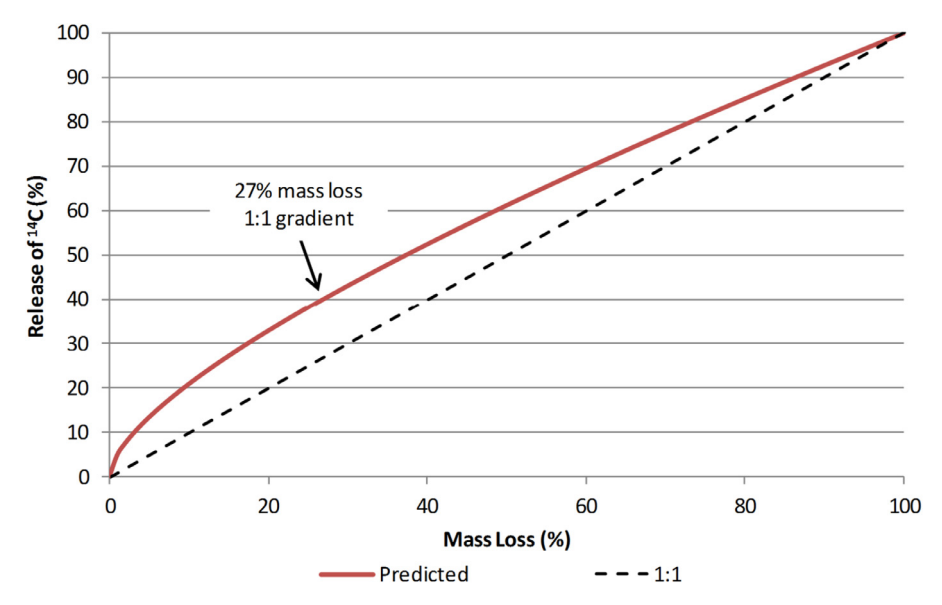


Fig. 6. The empirically-derived predicted ¹⁴C release profile for this source of irradiated graphite, with demonstrative 1:1 ¹⁴C to mass loss line.

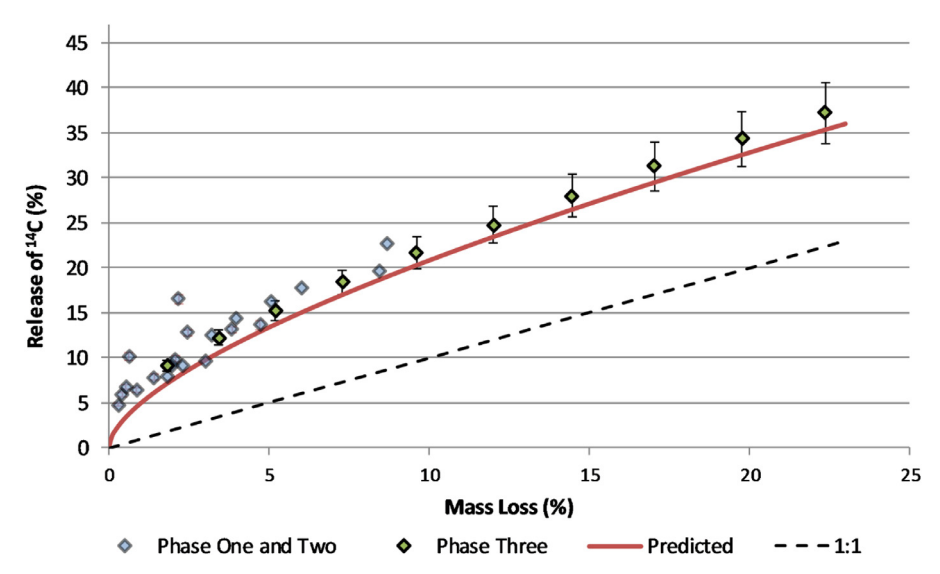


Fig. 7. The 14C release profile for samples treated at 600°C inclusive of single treatment and consecutive treatment experimental data.

enriched region did not exist and all of the ^{14}C were randomly distributed throughout the graphite specimens. A sensitivity study has been performed which considers the standard deviation in the data after solving the simultaneous equations with the data points not selected, suggesting a confidence interval (1σ) of $\pm 7\%$ absolute is appropriate for a predictive trend derived using Figure 3. The ^{14}C to ^{12}C selective removal efficiency is initially high, falling from 5:1 to 3:1 in the first 1% of mass loss. Comparison of the gradient of the predicted curve with the 1:1 line suggests that if this trend holds true into larger mass losses, then a ^{14}C to ^{12}C removal efficiency of greater than 1 can be maintained until approximately 27% thermal mass loss, though the efficiency of that removal reduces considerably as treatment progresses.

The empirically predicted function presented in Figure 6 can be compared to both the data from Figure 2, from which it is derived, and the ¹⁴C release results from the Phase Three consecutive testing of a single sample to larger mass losses, which do not contribute to the derivation of the predictive function. This comparison can be seen graphically in Figure 7. The release data for the consecutively treated sample and the predictive function

are very similar in profile, giving confidence that the data collected for smaller mass losses can be extrapolated in this manner, and that the ¹⁴C release profile is predictable between samples. This release profile also appears to correspond well with the compilation of multiple sources of thermal treatment provided by Metcalfe et al.[43], suggesting that the relationship holds true to greater sample mass losses than seen in this study. This relationship also confirms that a ¹⁴C release to mass loss ratio greater than 1:1 can be maintained to significant mass losses, including in this instance until catastrophic loss of sample structural integrity, suggesting that there is a ¹⁴C concentration distribution to a significant depth into the pore walls and bulk material. Despite falling mostly within the uncertainties on the data, the predicted profile is consistently below the release data in Figure 7, suggesting that the principle holds true but there is scope for improving the predictive function to more accurately predict absolute release fractions. Some discrepancy between prediction and data could also be caused by sample inhomogeneity, whereby a sample has a greater or lesser proportion of surface region ¹⁴C and thus that release profile will quickly become offset in the y-axis as the surface region ^{14}C oxidised early in the treatment is depleted at a different rate.

One interesting observation that can be drawn from Figure 6 is that at 27% mass loss, where approximately 40% of the total ¹⁴C content has been released from the sample, the ¹⁴C-enriched surface region is almost entirely depleted and approximately 27% of any randomly distributed ¹³C-derived ¹⁴C component will also have been released from the sample. By simple subtraction, this suggests that the ¹⁴C-enriched surface layer is responsible for just 13% of the entire ¹⁴C inventory of a sample. Therefore, a considerably larger fraction of the ¹⁴C content in these samples is randomly distributed through the bulk material and cannot be preferentially removed using low temperature thermal oxidation of solid specimens. It should be duly noted that, due to in-reactor processes such as radiolytic oxidation removing significant quantities of surface material from the pore surfaces throughout the lifetime of the material, these data are not equivalent to a prediction of the location of the entirety of the 14C formation in these samples, but more a representation of its location in these samples as-received.

Care should be taken, with application of these data to alternative sources of graphite, including from different regions of a reactor core, different reactors, different reactor designs, and grades of graphite, as all of these and the associated neutron fluxes, graphite microstructures and nitrogen distributions will influence the formation and removability of ¹⁴C. This could explain why similar processes are more efficient for graphite sourced from RBMK reactors where the graphite is irradiated in a helium-nitrogen atmosphere, without the corrosive radiolytic oxidation processes of CO₂-cooled reactors. Conversely, in an accident scenario or long-term storage RBMK graphite could be more susceptible to release of this surface region ¹⁴C than UK Magnox reactor graphites.

Defining the threshold at which the selective 14C release efficiency becomes viable for a large-scale graphite treatment programme is outside the scope of this paper, though the majority of any beneficial effects are lost by approximately 5% mass loss. The absolute release fractions with mass loss observed in this work are similar in magnitude, though slightly lower than, those observed by Pageot et al.[44] studying crushed UNGG samples in elevated temperature CO₂. One would expect that crushing samples would dilute any ¹⁴C-enriched surface regions with fresh ¹²C surfaces, reducing the effectiveness of any treatment as observed by Fachinger et al.[40], though the effects of any remaining 14C-enriched surfaces, if there were any, could still contribute to the overall release profile. Although the ¹³C-derived component has been treated as randomly distributed and 'locked in' during this work, the work by Pageot et al.[44] suggests that there could also be scope to selectively extract a fraction of that component by alternative means. It should be noted that an important advantage of the method demonstrated in this paper, both for determining a ¹⁴C release profile with mass loss for a given material and adoption of the method for treatment, is the retention of solid specimens, which improves ease of handling and reduces the need to mitigate for airborne powder and dust generation through crushing or milling. There is limited evidence that changing the concentration of oxygen in the oxidising gas could influence the ¹⁴C removal efficiency [13] and so further experiments with concentrations of oxygen other than 1%, or application of 1% oxygen to alternative sources of graphite, could be beneficial. There could be significant economic advantages to employing compressed air as an oxidising gas, if this was not detrimental to selective removal of ¹⁴C.

Conclusion

A method of establishing a ¹⁴C release profile in graphite with progressive surface mass loss by repeated discrete measurements has been presented, with good resolution of ¹⁴C release character-

istics in the low mass gain region and offering good confidence in the results by demonstrating uniformity in behaviour between 22 similarly sourced reactor samples. This comes at the expense of time, number of samples undergoing destructive testing and representativeness to alternative sources of graphite, though is the first work to construct a ¹⁴C release profile in such detail. An empirical prediction for the ¹⁴C release behaviour with mass loss has been derived from thermal treatment data of Oldbury Magnox reactor sourced graphite which is demonstrated to hold true to larger sample mass losses. This suggests that despite the natural inhomogeneity of irradiated graphite specimens the ¹⁴C release profile from similarly sourced irradiated graphite material is empirically predictable and repeatable.

This work has contributed evidence that the 14C-enriched surface region persists to far deeper in these irradiated graphite samples than can be solely attributed to a surface carbonaceous deposit. It has been shown using low temperature thermal oxidation to effect oxidation throughout the surfaces of the open porosity that an accelerated rate of ¹⁴C release is achieved at smaller sample mass losses, the efficiency of which diminishes with additional mass loss. This is indicative of release of a concentration gradient of ¹⁴C from the gas-facing surfaces inwards, likely including contributions from the carbonaceous deposit, underlying ¹⁴N-derived ¹⁴C and a fraction of randomly distributed ¹³C-derived ¹⁴C. The release profile becomes more linear with increasing mass loss as randomly distributed ¹³C-derived ¹⁴C release from the bulk material of the sample dominates. For these samples, a ¹⁴C release to mass loss percentage ratio of greater than 1 can be maintained until approximately 27% mass loss, and only an estimated 13% of the total ¹⁴C inventory in these samples as-received can be attributed to a ¹⁴C-enriched surface region, though this fraction is likely to vary between positions in the core and precise irradiation histories.

This work demonstrates a novel method for determining the distribution of ¹⁴C between near-surface regions and the bulk material in differing sources of irradiated graphite, which could be used for graphite specimens from different regions of a core, or different reactors, to empirically determine the distribution at those locations. The data generated could then inform decision making for the adoption of a wider programme of low temperature thermal treatment as an alternative radioactive waste management route for irradiated graphite.

Declaration of Competing Interest

The authors declare that they have no known competing financial interests or personal relationships that could have appeared to influence the work reported in this paper.

Acknowledgments

This work was supported by the Engineering and Physical Sciences Research Council (EPSRC), studentship award number 1241249 and the EU FP7 *CARBOWASTE* project (FP7-211333). The authors would also like to acknowledge Greg Black and Lorraine McDermott, for contributions and guidance early in this programme of research, and to thank the National Nuclear Laboratory for performing the carbonaceous deposit analysis. Lastly, much of the inspiration and motivation for this work has stemmed from *CARBOWASTE* and the IAEA CRP for *Treatment of Irradiated Graphite to Meet Acceptance Criteria for Waste Disposal* (CRP T21026).

References

- [1] Nuclear Decommissioning Authority, UK Radioactive Waste and Materal Inventory, 2019.
- [2] Nuclear Decommissioning Authority, Integrated Waste Management NDA Higher Activity Waste Strategy, 2016.

- [3] A.J. Wickham, G.B. Neighbour, M. Dubourg, in: The Uncertain Future for Nuclear Graphite Disposal: Crisis or Opportunity?, in: Proceedings of the Technical Committee on Nuclear Graphite Waste Management, 1999 Manchester.
- [4] G. Holt, Radioactive Graphite Management at UK Magnox Nuclear Power Stations, in: IAEA Technical Committee Meeting, 1999 Vienna.
- [5] G. Black, Doctoral Thesis: Irradiated Graphite Waste: Analysis and Modelling of Radionuclide Production With a View to Long Term Disposal, University of Manchester, 2014.
- [6] I.F. White, G.M. Smith, L.J. Saunders, C.J. Kaye, T.J. Martin, G.H. Clarke, M. Wakerley, Assessment of Management Modes for Graphite from Reactor Decommissioning, 1984 Commission of the European Communities.
- [7] International Atomic Energy Agency, Characterization, Treatment and Conditioning of Radioactive Graphite from Decommissioning of Nuclear Reactors, 2006 IAEA-TECDOC-1521, Vienna
- [8] A.R. Doyle, K. Hammond, The Estimation of Tritium, Sulphur-35 and Carbon-14 in Reactor Coolant Gas and Gaseous Effluents, in: IAEA-SM-245/33 International Symposium on Management of Gaseous Wastes from Nuclear Facilities, 1980, pp. 347-361. Vienna.
- [9] B.J. Marsden, K.L. Hopkinson, A.J. Wickham, The Chemical Form of Carbon-14 Within Graphite, 2002 Report SA/RJCB/RD03612001/R01 Issue 4. A Serco Assurance Report for NIREX.
- [10] M.P. Metcalfe, R.W. Mills, Radiocarbon Mass Balance for a Magnox Nuclear Power Station, Ann. Nucl. Energy. 75 (2015) 665-671, doi:10.1016/J.ANUCENE. 2014.08.071.
- [11] D. Ancius, D. Ridikas, V. Remeikis, A. Plukis, R. Plukiene, M. Cometto, Evaluation of the Activity of Irradiated Graphite in the Ignalina Nuclear Power Plant RBMK-1500 Reactor, Nukleonika 50 (2005) 113-120.
- [12] T. Podruzhina, Doctoral Thesis: Graphite as Radioactive Waste Corrosion Behaviour under Final Repository Conditions and Thermal Treatment, 2004 Forschungszentrum Jülich.
- [13] M. Dunzik-Gougar, T.E. Smith, Removal of Carbon-14 from Irradiated Graphite,
- J. Nucl. Mater. 451 (2014) 328–335, doi:10.1016/J.JNUCMAT.2014.03.018.
 [14] D. LaBrier, M. Dunzik-Gougar, Characterization of ¹⁴C in Neutron Irradiated NBG-25 Nuclear Graphite, J. Nucl. Mater. 448 (2014) 113-120, doi:10.1016/J. INUCMAT.2014.01.041
- [15] International Atomic Energy AgencyTreatment of Irradiated Graphite to Meet Acceptance Criteria for Waste Disposal, 2016 TECDOC-1790, Vienna.
- [16] D. Vulpius, K. Baginski, C. Fischer, B. Thomauske, Location and Chemical Bond of Radionuclides in Neutron-irradiated Nuclear Graphite, J. Nucl. Mater. 438 (2013) 163-177, doi:10.1016/j.jnucmat.2013.02.027.
- [17] D. Bradbury, A.J. Wickham, (Principal Authors), Carbon-14 in Irradiated Graphite Waste, 2010 Electric Power Research Institute, Palo Alto CA.
- [18] D. Vulpius, W. von Lensa, Determination of the Chemical Bond of Carbon-14 in Neutron-Irradiated Nuclear Graphite, Institute for Energy Research - Safety Research and Reactor Technology, 2009 (IEF-6) Report.
- [19] J.V. Best, W.J. Stephen, A.J. Wickham, Radiolytic Graphite Oxidation, Prog. Nucl. Energy. 16 (1985) 127-178, doi:10.1016/0149-1970(85)90002-2
- [20] M.P. Metcalfe, A. Tzelepi, J. Gill, Carbon-14 Content of Carbonaceous Deposits in Oldbury Core Graphite, 2016 in: IAEA-TECDOC-1790 Companion CD-ROM https://inis.iaea.org/collection/NCLCollectionStore/_Public/47/090/ 47090161.pdf (accessed 04/06/2021).
- [21] L. Payne, P.J. Heard, T.B. Scott, Examination of Surface Deposits on Oldbury Reactor Core Graphite to Determine the Concentration and Distribution of 14C, PLoS One 11 (2016), doi:10.1371/journal.pone.0164159.
- [22] B. Poncet, L. Petit, Method to Assess the Radionuclide Inventory of Irradiated Graphite Waste from Gas-cooled Reactors, J. Radioanal. Nucl. Chem. 298 (2013) 941-953, doi:10.1007/s10967-013-2519-6.
- [23] B. Poncet, EDF Radioactive Graphite Inventories Based on Hundreds of Measurements are Casting Doubt on "a Priori" Accepted Ideas, 2010 in: WM2010 Conf. March 7-11, Phoenix https://xcdsystem.com/wmsym/archives//2010/pdfs/ 10414.pdf (accessed 04/06/2021).
- [24] P.L. Walker, F. Rusinko, L.G. Austin, Gas Reactions of Carbon, Adv. Catal. 11 (1959) 133-221, doi:10.1016/S0360-0564(08)60418-6.
- [25] H.K. Hinssen, K. Kühn, R. Moormann, B. Schlögl, M. Fechter, M. Mitchell, Oxidation Experiments and Theoretical Examinations on Graphite Materials Relevant for the PBMR, Nucl. Eng. Des. 238 (2008) 3018-3025, doi:10.1016/j.nucengdes.
- [26] J. Liu, L. Dong, C. Wang, T. Liang, W. Lai, First Principles Study of Oxidation Behavior of Irradiated Graphite, Nucl. Instruments Methods Phys. Res. Sect. B Beam Interact, with Mater. Atoms. 352 (2015) 160-166, doi:10.1016/j.nimb.
- [27] R.H. Hurt, B.S. Haynes, On the Origin of Power-law Kinetics in Carbon Oxidation, Proc. Combust. Inst. (2005) 2161-2168 30 II, doi:10.1016/j.proci.2004.08.
- [28] S. Ahmed, M.H. Back, The Role of the Surface Complex in the Kinetics of the Reaction of Oxygen with Carbon, Carbon 23 (1985) 513-524, doi:10.1016/ 0008-6223(85)90087-9.
- [29] F.J. Vastola, P.J. Hart, P.L. Walker, A Study of Carbon-oxygen Surface Complexes using O18 as a Tracer, Carbon 2 (1964) 65-71, doi:10.1016/0008-6223(64) 90029-6.
- [30] J.A. Moulijn, F. Kapteijn, Towards a Unified Theory of Reactions of Carbon with Oxygen-containing Molecules, Carbon 33 (1995) 1155-1165, doi:10.1016/ 0008-6223(95)00070-T.

- [31] P.A. Campbell, R.E. Mitchell, The Impact of the Distributions of Surface Oxides and their Migration on Characterization of the Heterogeneous Carbon-oxygen Reaction, Combust. Flame. 154 (2008) 47-66, doi:10.1016/j.combustflame.2007.
- [32] T.J. Clark, R.E. Woodley, D.R. de Halas, Gas-Graphite Systems, in: R.E. Nightingale (Ed.), Nuclear Graphite, Academic Press, 1962, pp. 387–445, doi:10.1016/b978-1-4832-2854-9.50018-3. New York and London.
- [33] M.S. El-Genk, J.M.P. Tournier, Validation of Gasification Model for NBG-18 Nuclear Graphite, Nucl. Eng. Des. 250 (2012) 142-155, doi:10.1016/j.nucengdes. 2012 05 016
- [34] X. Luo, X. Yu, S. Yu, Oxidation Performance of Graphite Material in Reactors, Front. Energy Power Eng. China. 2 (2008) 471-474, doi:10.1007/ s11708-008-0074-6
- [35] C.I. Contescu, S. Azad, D. Miller, M.J. Lance, F.S. Baker, T.D. Burchell, Practical Aspects for Characterizing Air Oxidation of Graphite, J. Nucl. Mater. 381 (2008) 15-24, doi:10.1016/j.jnucmat.2008.07.020.
- W.L. Kosiba, G.J. Dienes, The Effect of Displaced Atoms and Ionizing Radiation on the Oxidation of Graphite, Adv. Catal. 9 (1957) 398-405, doi:10.1016/ S0360-0564(08)60191-1
- [37] O'Brien M.H., Merrill B.J., Ugaki S.N., Combustion Testing and Thermal Modeling of Proposed CIT (Compact Ignition Tokamak) Graphite Tile Materials, 1988 Report EGG-FSP-8255.
- [38] A. Theodosiou, A.N. Jones, B.J. Marsden, Thermal Oxidation of Nuclear Graphite: A Large Scale Waste Treatment Option, PLoS One (2017) 12, doi:10. 1371/journal.pone.0182860.
- [39] A.J. Wickham, Caring for the Graphite Cores, in: The Review of Safety at Magnox Installations, London, Institution of Mechanical Engineers CONF-8903273 (1991) 79-87.
- [40] J. Fachinger, W. von Lensa, T. Podruhzina, Decontamination of Nuclear Graphite, Nucl. Eng. Des. 238 (2008) 3086-3091, doi:10.1016/j.nucengdes.2008. 02.010
- [41] D. Vulpius, K. Baginski, B. Kraus, B. Thomauske, Thermal Treatment of Neutronirradiated Nuclear Graphite, Nucl. Eng. Des. 265 (2013) 294-309, doi:10.1016/j. nucengdes, 2013, 09, 007,
- [42] O.K. Karlina, M.A. Tuktarov, V.A. Kasheev, Methods of Irradiated Graphite Treatment - Characteristic Properties of Irradiated Graphite, in: IAEA-TECDOC-1790 Companion CD-ROM, 2016 https://inis.iaea.org/collection/ NCLCollectionStore/_Public/47/090/47090164.pdf (accessed 04/06/2021).
- [43] M.P. Metcalfe, A. Tzelepi, G. Copeland, The Release of Carbon-14 from Irradiated PGA Graphite by Thermal Treatment in Air, Ann. Nucl. Energy. 133 (2019) 110-121, doi:10.1016/j.anucene.2019.05.016.
- [44] J. Pageot, J.N. Rouzaud, L. Gosmain, A. Duhart-Barone, J. Comte, D. Deldicque, 14 C Selective Extraction from French Graphite Nuclear Waste by CO $_2$ Gasification, Prog. Nucl. Energy. 105 (2018) 279-286, doi:10.1016/j.pnucene.2018.02.
- [45] R.N. Worth, Doctoral Thesis: Thermal Treatment Of Oldbury Magnox Reactor Irradiated Graphite, University of Manchester, 2015
- [46] D.A. Wickenden, Carbolite Process Manual Analysis of Tritium and Carbon- 14 in Combustible Materials using the Carbolite/AEA Technology Combustion Furnace and Associated Apparatus, Carbolite and AEA Technology Report MF38PR,
- [47] International Atomic Energy Agencylrradiation Damage in Graphite due to Fast Neutrons in Fission and Fusion Systems, IAEA-TECDOC-1154, 2000 Vienna.
- [48] L. Xiaowei, R. Jean-Charles, Research of Oxidation Properties of Graphite Used in HTR-10, 2006 Report CNIC-01856/2006.
- [49] R. Moormann, H.K. Hinssen, K. Kühn, Oxidation Behaviour of an HTR Fuel Element Matrix Graphite in Oxygen Compared to a Standard Nuclear Graphite, Nucl. Eng. Des. (2004), doi:10.1016/j.nucengdes.2003.11.001.
- [50] E.A. Gulbransen, K.F. Andrew, F.A. Brassart, The Oxidation of Graphite at Temperatures of 600° to 1500°C and at Pressures of 2 to 76 Torr of Oxygen, J. Electrochem. Soc. (1963), doi:10.1149/1.2425797.
- [51] W. Lu, X. Li, X. Wu, L. Sun, Z. Li, Investigation on the Oxidation Behavior and Multi-step Reaction Mechanism of Nuclear Graphite SNG742, J. Nucl. Sci. Technol. (2020), doi:10.1080/00223131.2019.1671910.
- C.M. Tu, H. Davis, H.C. Hottel, Combustion Rate of Carbon: Combustion of Spheres in Flowing Gas Streams, Ind. Eng. Chem. (1934), doi:10.1021/
- [53] L. Payne, P.J. Heard, T.B. Scott, A Study of the Oxidation Behaviour of Pile Grade A (PGA) Nuclear Graphite using Thermogravimetric Analysis (TGA), Scanning Electron Microscopy (SEM) and X-ray Tomography (XRT), PLoS One (2015), doi:10.1371/journal.pone.0143041.
- [54] G.F. Hewitt, M.J.C. Moore, E.W. Sharratt, The Diffusion of Oxygen in Nitrogen in the Pores of Graphite: The Effect of Oxidation on Diffusivity and Permeability, Carbon (1970), doi:10.1016/0008-6223(70)90068-0.
- [55] M.A. Kanter, Diffusion of Carbon Atoms in Natural Graphite Crystals, Phys. Rev. 107 (1957) 655-663, doi:10.1103/PhysRev.107.655.
- [56] R.S. Sach, W.J. Williams, The Diffusion of ¹⁴C in Nuclear Graphites, Carbon 12 (1974) 425-432, doi:10.1016/0008-6223(74)90008-6.